Six-Membered Spirocycle Triggered Probe for Visualizing Hg^{2+} in Living Cells and Bacteria−EPS−Mineral Aggregates

Zheng Yang,[†,||] Likai Hao,[‡,||] Bing Yin,[†,§] Mengyao She,[†] Martin Obst,[‡] Andreas Kappler,[‡] and Jianli Li*,[†]

Ministry of Education Key Laboratory of Synthetic and Natural Functional Molecule Chemistry, College of Chemistry & Materials Science, Northwest University, Xi'an, Shaanxi 710069, P. R. China, Center for Applied Geoscience, Institute for Geoscience, Eberhard Karls University Tuebingen, Hoelderlinstr. 12, Tuebingen 72074, Germany, and College of Chemistry, Beijing Normal University, No. 19, XinJieKouWai Street, HaiDian District, Beijing 100875, P. R. China

lijianli@nwu.edu.cn

ABSTRACT
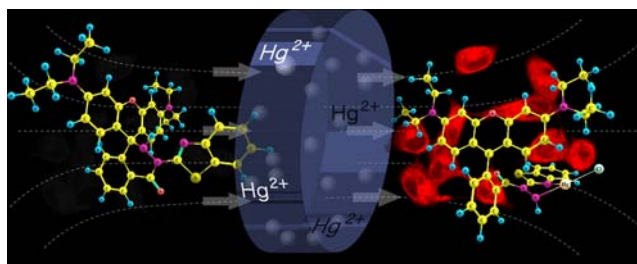
A novel rhodamine based probe with a unique six-membered spirocycle was rationally designed for detection of Hg^{2+} with greatly improved selectivity, sensitivity, and photostability. The probe has been shown to be suitable for Hg^{2+} imaging in living cells and mapping Hg^{2+} distribution in living cell−EPS−mineral aggregates under anoxic conditions.

Mercury has been known as one of the most ubiquitous and hazardous pollutants in nature.[1] Methods are required for mapping and quantifying Hg^{2+} in biological samples. Fluorescence staining has advantages of high sensitivity and spatial resolution in combination with, in microscopy, being nondestructive to the samples and less cell-damaging.[2] By virtue of the desirable properties,[3] excellent examples of rhodamine based fluorescent probes have been developed for biologically relevant metal species on the basis of an ion-induced ring-opening process.[4]

Reported Hg^{2+} probes usually contain a five-membered spirolactam moiety.[5] In general, an appropriate ligand at the spirolactam ring can induce color and fluorescence changes by activating the carbonyl group upon binding of metal ions. However, the application of these probes is limited by weak fluorescence intensity, short fluorescence stability, and even fluorescence quenching.[6] These drawbacks can potentially be addressed by expanding beyond a

[†] Northwest University.
[‡] Eberhard Karls University Tuebingen.
[§] Beijing Normal University.
[||] Z.Y. and L.K.H. contributed equally to this work.

(1) (a) Kong, I. C.; Bitton, G.; Koopman, B.; Jung, K. H. *Rev. Environ. Contam. T.* **1995**, *142*, 119. (b) Tan, S. W.; Meiller, J. C; Mahaffey, K. R. *Crit. Rev. Toxicol.* **2009**, *39*, 228.

(2) (a) Thomas, S. W., III; Joly, G. D.; Swager, T. M. *Chem. Rev.* **2007**, *107*, 1339. (b) Du, J. J.; Hu, M. M.; Fan, J. L.; Peng, X. J. *Chem. Soc. Rev.* **2012**, *41*, 4511. (c) Yang, X. F.; Guo, Y. X.; Strongin, R. M. *Angew. Chem., Int. Ed.* **2011**, *50*, 1.

(3) Ramette, R. W.; Sandell, E. B. *J. Am. Chem. Soc.* **1956**, *78*, 4872.

(4) (a) Niu, L. Y.; Guan, Y. S.; Chen, Y. Z.; Wu, L. Z.; Tung, C. H.; Yang, Q. Z. *J. Am. Chem. Soc.* **2012**, *134*, 18928. (b) Michel, B. W.; Lippert, A. R.; Chang, C. J. *J. Am. Chem. Soc.* **2012**, *134*, 15668. (c) Hirayama, T.; Okuda, K.; Nagasawa, H. *Chem. Sci.* **2013**, *4*, 1250.

(5) (a) Chen, X. Q.; Pradhan, T.; Wang, F.; Kim, J. S.; Yoon, J. *Chem. Rev.* **2012**, *112*, 1910. (b) Yang, Y. M.; Zhao, Q.; Feng, W.; Li, F. Y. *Chem. Rev.* **2013**, *113*, 192. (c) Ko, S.; Yang, Y.; Tae, J.; Shin, I. *J. Am. Chem. Soc.* **2006**, *128*, 14150. (d) Yang, K.; Zhou, Z. G.; Huang, K. W.; Yu, M. X.; Li, F. Y.; Yi, T.; Huang, C. H. *Org. Lett.* **2007**, *9*, 4729. (e) Du, J. J.; Fan, J. L.; Peng, X. J.; Sun, P. P.; Wang, J. Y.; Li, H. L.; Sun, S. G. *Org. Lett.* **2010**, *12*, 476.

(6) (a) Zhang, X. L.; Xiao, Y.; Qian, X. H. *Angew. Chem., Int. Ed.* **2008**, *47*, 8025. (b) Shi, W.; Ma, H. M. *Chem. Commun.* **2008**, 1856. (c) Xi, P. X.; Huang, L.; Xie, G. Q.; Chen, F. J.; Xu, Z. H.; Bai, D. C.; Zeng, Z. Z. *Dalton Trans.* **2011**, *40*, 6382.

five-membered spirocycle. At present, the development of highly sensitive and clinically applicable diagnostic methods for Hg^{2+} has attracted great attention.[7]

Among the most attractive methodological innovations, expansion of the spirocycle has the potential to improve the stability of the probe while providing more binding positions, thus potentially improving the selectivity and fluorescent properties.[8] Although our group and others have devoted much effort toward enlarging the spirocycle to a six-member moiety, few satisfying products have been demonstrated to date.
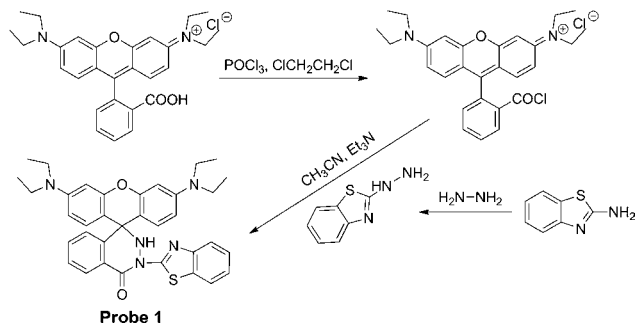

Figure 1. Synthesis of rhodamine based probe **1**.

Herein we describe the design and application of a hydrazinobenzothiazole based six-membered probe **1** (Figure 1). The nonplanar six-membered spirocycle in **1** has been proven to be well suited for the recognition of Hg^{2+} with improved optical properties relative to reported probes.[6,9] Furthermore, prolonged fluorescence stability indicated a significant resistance to irreversible photobleaching. The wonderful multilabeling properties make **1** highly suitable for the mapping of Hg^{2+} distribution in living cell−EPS−mineral aggregates, which may provide breakthrough insight into the correlation between Hg^{2+} and organic substances such as cells, microbes, and biofilms. To the best of our knowledge, this is the first six-membered spirocycle fluorescent probe which displays such promising properties for Hg^{2+} detection.

As expected, probe **1** is colorless and emits no fluorescence in ethanol−PBS (4/6, v/v, pH 7.4) solution. Notably, upon addition of Hg^{2+}, an intense absorption band centered at 556 nm (Figure 2a), coupled with a brilliant pink coloration. Concomitantly, a strong orange emission band appeared around 574 nm (Figure 2b) with a high fluorescent quantum yield ($\Phi = 0.87$). Fluorescent titration with 20 μM of **1** demonstrated that the detection limit was
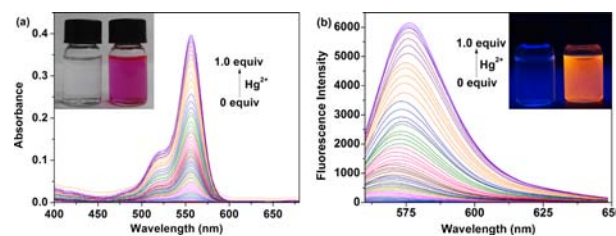

Figure 2. Fluorescence intensity (a) and absorption (b) changes of **1** (20 μM) upon addition of Hg^{2+} (0−1.5 equiv) in ethanol−PBS (4/6, v/v, pH 7.4) solution (excitation at 550 nm).

30 nM. About 1.0 equiv of Hg^{2+} was required until a plateau was reached with the fluorescence intensity increased for more than 1000-fold. Under these conditions, a linear correlation between **1** and the concentration of Hg^{2+} ranged from 30 nM to 20 μM, indicating the suitability for quantitative determination of Hg^{2+} (Figure S3).

The fluorescence intensity in the presence of Hg^{2+} was compared to other metals to study the selectivity of **1** and the competition caused by other ions (Figure 3). The probe showed excellent selectivity to Hg^{2+} with dramatic absorbance and fluorescence changes, whereas other metal ions showed insignificant responses. Only Ag^+ had a slight effect which is significantly inferior and easily quenched. Variation of the Hg^{2+} counterion had negligible effects on the fluorescence intensity. The competition experiments which were carried out by adding Hg^{2+} to the **1** solution in the presence of other metal ions revealed that the selectivity of **1** to Hg^{2+} did not significantly experience interference from the commonly coexistent ions, although Ag^+, Cu^{2+}, and Fe^{3+} induced slight fluorescent quenching or enhancement.
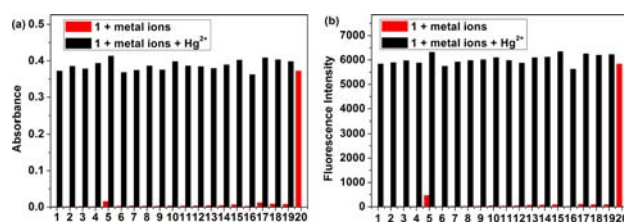

Figure 3. Absorption (a) and fluorescence intensity (b) changes of **1** (20 μM) upon the addition of various metal ions (20 μM) in ethanol−PBS (4/6, v/v, pH 7.4) solution. Red bars represent the fluorescence response of **1** to the metal ions of interest. 1, blank; 2, Li^+; 3, Na^+; 4, K^+; 5, Ag^+; 6, Ba^{2+}; 7, Ca^{2+}; 8, Mg^{2+}; 9, Cd^{2+}; 10, Mn^{2+}; 11, Co^{2+}; 12, Fe^{2+}; 13, Ni^{2+}; 14, Zn^{2+}; 15, Pb^{2+}; 16, Cu^{2+}; 17, Fe^{3+}; 18, Cr^{3+}; 19, Al^{3+}; 20, Hg^{2+}. Black bars represent the subsequent addition of Hg^{2+} (20 μM) to the above solutions (excitation at 550 nm; emission at 574 nm).

Microcalorimetry was used for a better understanding of the mechanism.[10] The enthalpy at 298.15 K was measured to be -24.09 ± 0.02 kJ/mol, revealing that the

(7) (a) Ando, S.; Koide, K. *J. Am. Chem. Soc.* **2011**, *133*, 2556. (b) Yang, M.; Thirupathi, P.; Lee, K. *Org. Lett.* **2011**, *13*, 5028. (c) Vedamalai, M.; Wu, S. P. *Org. Biomol. Chem.* **2012**, *10*, 5410.

(8) Wu, C.; Bian, Q. N.; Zhang, B. G.; Cai, X.; Zhang, S. D.; Zheng, H.; Yang, S. H.; Jiang, Y. B. *Org. Lett.* **2012**, *14*, 4198.

(9) (a) Wang, J. B.; Qian, X. H. *Chem. Commun.* **2006**, 109. (b) Li, D.; Wieckowska, A.; Willner, I. *Angew. Chem., Int. Ed.* **2008**, *47*, 3927. (c) Shiraishi, Y.; Sumiya, S.; Kohno, Y.; Hirai, T. *J. Org. Chem.* **2008**, *73*, 8571. (d) Kumar, M.; Kumar, N.; Bhalla, V.; Singh, H.; Sharma, P. R.; Kuar, T. *Org. Lett.* **2011**, *13*, 1422.

(10) (a) Cardona-Martinez, N.; Dumesic, J. A. *Adv. Catal.* **1992**, *38*, 149. (b) Gaisford, S. *Adv. Drug Delivery Rev.* **2012**, *64*, 431.

ring-opening process is exothermic and spontaneous. Job's plot showed a 1:1 stoichiometry between **1** and Hg^{2+} with an association constant of $1.02 \times 10^6 \ M^{-1}$, indicating the strong binding affinity of **1** to Hg^{2+} (Figure S5). The mass spectrum manifested a peak at m/z 826.1943, assigned as $[\mathbf{1} + Hg^{2+} + Cl^-]^+$, providing further evidence for the binding mode. The absorption at $1678 \ cm^{-1}$ in IR analysis did not shift to lower frequency upon addition of Hg^{2+} (Figure S10), indicating the carbonyl moiety was not involved in the coordination. Delightfully, a single crystal of the possible intermediate was obtained, and it suggested that the coordination of the Hg^{2+} selectively occurred at the N atoms of the hydrazine unit and benzothiazole moiety.

To better understand the binding between Hg^{2+} and **1**, DFT[11]-NBO analysis[12] focusing on the electron lone pairs (LP) was performed for **1**.[12] The LP of the N atoms of the hydrazine and benzothiazole moieties were computed to be the most possible ones to interact with Hg^{2+} (Figure S16). Based on these results, the most possible structure of the complex $[\mathbf{1} + Hg^{2+} + Cl^-]^+$ was proposed and validated by its lower energy compared to other possible structures (Figure S17). It can be concluded that the coordination of Hg^{2+} to the N atoms of the hydrazine and benzothiazole moieties reasonably promoted the opening of the spirocycle thus inducing the color and fluorescent changes (Figure 4).
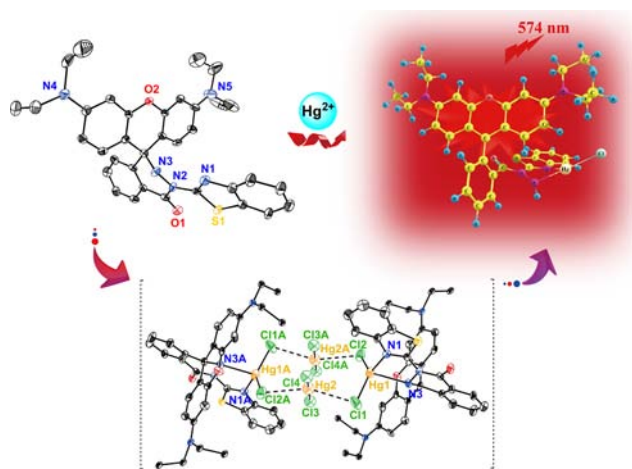

Figure 4. Proposed recognition process for the fluorescent changes upon addition of Hg^{2+}.

The absorption and fluorescent emission of the complex were theoretically modeled at the TDDFT[13] level based on the optimized structure of the ground S_0 state and the first excited S_1 state. The theoretical result was consistent with the experimental observation of strong fluorescence upon addition of Hg^{2+}. Both the absorption and emission corresponded mainly to the orbital transition between HOMO and LUMO (Figure 5). These frontier MOs were almost entirely distributed within the xanthene moiety absolutely and thus the corresponding dipole integral would be large. Finally the transition dipole moment between the S_0 and S_1 states was large as well as the strengths of the corresponding absorption and emission. Although the calculations underestimate the absorption wavelength by ∼70 nm, the theoretical emission wavelength 543 nm was quite close to the experimental value (within ∼30 nm). As shown in Figure 5, the Stokes shift mainly arose from the lower LUMO energy (−3.17 ev) induced by the geometry relaxation at the potential energy surface of the S_1 state.

The fluorescent response changed inappreciably in the pH range of 4−8 (Figure S6) and had little interference from sulfur compounds (Figure S7). This is highly desirable for quantifying Hg^{2+} in biological systems. As a proof-of-concept, HeLa cells were pretreated with 20 μM of **1** or vehicle control for 4 h at 37 °C and then incubated with 20 μM $HgCl_2$ in the same culture medium. The preliminary experiments in HeLa cells demonstrated that **1** is especially suited for *in vivo* imaging (Figure S8).
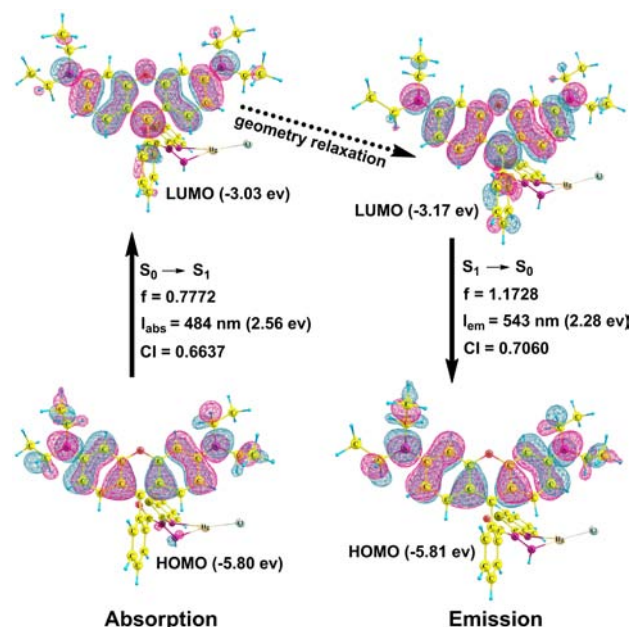

Figure 5. Theoretical wavelength (λ), excitation energy, oscillator strength (f), relevant frontier MOs (3D distribution and orbital energy), and corresponding CI coefficient of the absorption and emission of the complex $[\mathbf{1} + Hg^{2+} + Cl^-]^+$ in ethanol solvent.

Probe **1** was then used to map the sorption of Hg^{2+} to bacteria−EPS−mineral aggregates under anoxic conditions[14] (Figure S8). Reflection images of bacteria−EPS−mineral

(11) (a) Parr, R. G.; Yang, W. *Density Functional Theory of Atoms and Molecules*; Oxford University Press: New York, 1989. (b) Becke, A. D. *J. Chem. Phys.* **1993**, *98*, 5648.

(12) (a) Reed, A. E.; Curtiss, L. A.; Weinhold, F. *Chem. Rev.* **1988**, *88*, 899. (b) Yin, B.; Huang, Y. H.; Wang, G.; Wang, Y. *J. Mol. Model.* **2010**, *16*, 437.

(13) (a) Runge, E.; Gross, E. K. *Phys. Rev. Lett.* **1984**, *52*, 997. (b) Dreuw, A.; Head-Gordon, M. *Chem. Rev.* **2005**, *105*, 4009.

(14) (a) Hegler, F.; Posth, N. R.; Jiang, J.; Kappler, A. *FEMS Microbiol. Ecol.* **2008**, *66*, 250. (b) Miot, J.; Benzerara, K.; Obst, M.; Kappler, A.; Hegler, F.; Schadler, S.; Bouchez, C.; Guyot, F.; Morin, G. *Appl. Environ. Microb.* **2009**, *75*, 5586.
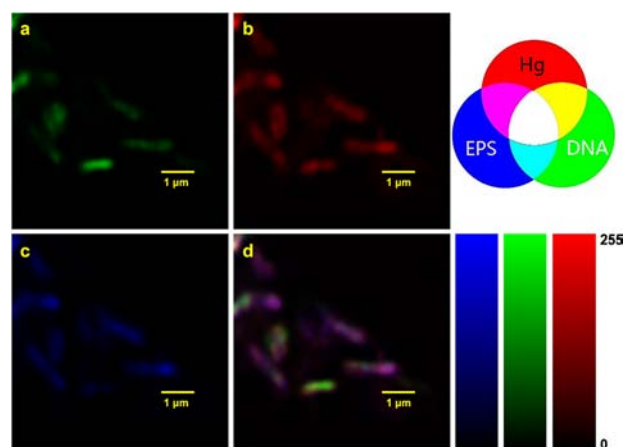
Figure 6. Single cell scale map the sorption of mercury to bacteria−EPS−mineral aggregates incubated with 20 μM Hg^{2+}. Simultaneously incubated sample with 20 μM probe **1** (b), fluorescent nucleic acid stain (a), and lectin conjugate (c) for 3 h at 20 °C (λ_{ex} = 488, 561, 635 nm). The overlay image of (a), (b), and (c) is shown in (d).

aggregates showed the morphological diversity. The overlay of fluorescence and reflection images revealed that Hg^{2+} was mainly adsorbed on the cells' surfaces. To better understand the mechanism and site of binding, DNA- and polysaccharide-specific fluorescent dyes[15] were applied simultaneously with **1** (Figure 6). On a single cell level, we show that capsule-like EPS structures enclose the SW2 cell. The structures were collocated with the fluorescence signal of **1** which indicated the Hg^{2+} adsorption to the EPS. The overlay image indicated that high concentrations of Hg^{2+} were located in the capsule-like EPS structure. This seemed to provide binding sites for Hg^{2+} and thus might protect the cell from mercury toxicity. Our results indicated that **1** could be used to map Hg^{2+} distribution in living cell−EPS−mineral aggregates under anoxic conditions. In comparison to other analytical approaches, fluorescence labeling has the advantage of analyzing the samples in an close to natural, hydrated state and thus avoids artifacts from sample preparation such as relocation of metals and dissolution/removal of EPS due to washing steps as they are required for electron microscopy sample preparation. Moreover, the approach could be a powerful tool to selectively screen bacterial strain and microbial biofilms for efficient removal of mercury from contaminated environments.

In summary, we developed a rhodamine derivative **1** with a unique six-membered spirocycle as a novel probe for Hg^{2+}. The extension of the spirocycle from a five- to a stretched nonplanar six-member ring greatly improved the properties of **1**, especially in terms of selectivity, sensitivity, and photostability. The recognition behaviors are investigated both experimentally and computationally. Introduction of the benzothiazole moiety has been proven to facilitate the formation of the six-membered spirocycle and the selective recognition of Hg^{2+}. Confocal laser scanning microscopy results show the applicability of **1** for multilabeling approaches. This should contribute to a significant breakthrough in understanding the correlation between Hg^{2+} and related cells and organic substances. More importantly, this probe is also a promising candidate for super-resolution fluorescence imaging with a lateral resolution of ∼20 nm using direct stochastic optical reconstruction microscopy.[16]

Supporting Information Available. Experimental details, optical spectra, IR, NMR, MS spectra, and computational details. This material is available free of charge via the Internet at http://pubs.acs.org.

(15) (a) Neu, T. R.; Lawrence, J. R. *FEMS Microbiol. Ecol.* **1997**, *24*, 11. (b) Peltola, M.; Neu, T. R.; Raulio, M.; Kolari, M.; Salkinoja-Salonen, M. S. *Environ. Microbiol.* **2008**, *10*, 1752. (c) Neu, T. R.; Manz, B.; Volke, F.; Dynes, J. J.; Hitchcock, A. P.; Lawrence, J. R. *FEMS Microbiol. Ecol.* **2010**, *72*, 1. (d) Zippel, B.; Neu, T. R. *Appl. Environ. Microb.* **2011**, *77*, 505.

(16) van de Linde, S.; Loeschberger, A.; Klein, T.; Heidbreder, M.; Wolter, S.; Heilemann, M.; Sauer, M. *Nat. Protoc.* **2011**, *6*, 991.